Diffusion MRI Characteristics After Concurrent Radiochemotherapy Predicts Progression-Free and Overall Survival in Newly Diagnosed Glioblastoma

Warren Chang[1], Whitney B. Pope[1], Robert J. Harris[1,2], Anthony J. Hardy[1,2], Kevin Leu[1,5], Reema R. Mody[3,6], Phioanh L. Nghiemphu[3,6], Albert Lai[3,6], Timothy F. Cloughesy[3,6], and Benjamin M. Ellingson[1,2,4,5,6]

Departments of [1]Radiological Sciences, [2]Biomedical Physics, [3]Neurology, and [4]Psychiatry and Biobehavioral Sciences, David Geffen School of Medicine; [5]Department of Bioengineering, Henry Samueli School of Engineering and Applied Science; and [6]Neuro-Oncology Program, University of California, Los Angeles, Los Angeles, CA

Corresponding Author:
Benjamin M. Ellingson, PhD
Departments of Radiological Sciences and Psychiatry, David Geffen
School of Medicine, University of California, Los Angeles,
924 Westwood Blvd, Suite 615, Los Angeles, CA 90024;
E-mail: bellingson@mednet.ucla.edu

ABSTRACT

The standard of care for newly diagnosed glioblastoma (GBM) is surgery first, radiotherapy (RT) with concurrent temozolomide (TMZ) second, and adjuvant TMZ last. We hypothesized patients with low diffusivity measured using apparent diffusion coefficient (ADC) histogram analysis evaluated after RT + TMZ and before adjuvant TMZ would have a significantly shorter progression-free survival (PFS) and overall survival (OS). To test this hypothesis, we evaluated 120 patients with newly diagnosed GBM receiving RT + TMZ followed by adjuvant TMZ. Magnetic resonance imaging was performed after completing RT + TMZ and before initiating adjuvant TMZ. A double Gaussian mixed model was used to describe the ADC histograms within the enhancing tumor, where ADC$_L$ and ADC$_H$ were defined as the mean ADC value of the lower and higher Gaussian distribution, respectively. An ADC$_L$ value of 1.0 μm^2/ms and ADC$_H$ value of 1.6 μm^2/ms were used to stratify patients into high- and low-risk categories. Results suggested that patients with a low ADC$_L$ had a significantly shorter PFS (Cox hazard ratio = 0.12, P = .0006). OS was significantly shorter with low ADC$_L$ tumors, showing a median OS of 407 versus 644 days (Cox hazard ratio = 0.31, P = .047). ADC$_H$ did not predict PFS or OS when accounting for age and ADC$_L$. In summary, after completing RT + TMZ, newly diagnosed glioblastoma patients with a low ADC$_L$ are likely to progress and die earlier than patients with a higher ADC$_L$. ADC histogram analysis may be useful for patient-risk stratification after completing RT + TMZ.

INTRODUCTION

Glioblastoma (GBM) is the most common and deadly form of primary brain tumors in adults. The current standard—aggressive therapy consisting of maximal surgical resection followed by concurrent radiotherapy (RT), temozolomide (TMZ) chemotherapy, and adjuvant TMZ—has shown a median survival of only 14.6 months (1-3). Although GBMs generally have a very poor prognosis, there are clearly cohorts of patients that benefit from specific therapies. Thus, there is great interest in identifying risk factors and biomarkers for predicting response to therapy beforehand. Patient age at diagnosis, neurological performance status, extent of surgical resection, radiographic composition of the tumor, tumor volume and location, isocitrate

dehydrogenase 1 mutation status, gene expression subtype, and O6-methylguanine methyltransferase promoter methylation are commonly assessed prognostic characteristics for GBM (4-12).

The use of imaging features to phenotype tumors and to predict therapeutic response is an attractive option compared with more invasive approaches based on tissue-derived biomarkers. By noninvasively characterizing the composition of the tumor microenvironment, features associated with particular response patterns can be identified that lead to the potential for patient cohort enrichment for use in clinical trials. We recently showed that the apparent diffusion coefficient (ADC) characteristics measured using diffusion magnetic resonance imaging (MRI) techniques can be used to predict both progres-

Figure 1. Treatment and MRI evaluation timeline. Patients were treated with 60 Gy of external beam radiation therapy (2-Gy fractions given once daily for 5 days over a 6-week period) with concomitant TMZ (75 mg/m^2 orally or intravenously for 42 consecutive days), followed by a 28-day break and then the start of adjuvant TMZ (150 mg/m^2 orally or intravenously for 5 consecutive days during the first 28-day cycle, followed by 200 mg/m^2 orally or intravenously for 5 consecutive days during the first 28-day cycle for a maximum of 6 cycles). Diffusion and standard anatomical MRI were performed within 10 weeks after the start of RT + TMZ or within 4 weeks from the end of RT + TMZ—just before adjuvant TMZ.

sion-free survival (PFS) and overall survival (OS) in GBM patients treated with bevacizumab at recurrence (13-15). Specifically, results in both single and multicenter trials have shown high ADC measurements within the contrast-enhancing tumor regions predict a favorable response to bevacizumab treatment at recurrence as indicated by a longer PFS and OS, whereas patients with low ADC measurements have a significantly shorter PFS and OS. It is important to note that results have also suggested that the prognostic capabilities of ADC measurements may be specific to bevacizumab therapy at recurrence, because no difference in PFS or OS were noted in bevacizumab-naïve patients treated with chemotherapy at recurrence (13). However, it is conceivable that ADC measurements may also be prognostic when used to evaluate the phase of adjuvant TMZ before the first recurrence, because various studies have suggested a general increase in ADC after successful RT + TMZ (16-21).

In this study, we examined a cohort of 120 patients with a newly diagnosed GBM that underwent tumor resection followed by RT + TMZ. We then evaluated the diffusion MRI characteristics within the tumor 4 weeks after completing RT+TMZ—just before starting the adjuvant phase of TMZ therapy. We hypothesized that high ADC measurements within contrast-enhancing voxels after completing RT + TMZ would indicate a longer PFS and OS.

METHODOLOGY
Patient Characteristics
All patients participating in this study signed institutional review board-approved informed consent. Data acquisition was performed in compliance with all applicable Health Insurance Portability and Accountability Act regulations. Patients were retrospectively selected from our institution's neuro-oncology database. Initially, a total of 169 patients who met the following criteria were selected: (1) pathology-confirmed glioblastoma, (2) treatment with standard external beam radiotherapy and concurrent TMZ followed by adjuvant TMZ, and (3) MRI scans obtained after surgical resection and within 4 weeks after RT + TMZ—just before the adjuvant phase of TMZ. The average age for this population was 58.4 years (±11-year SD), the average Karnofsky performance status score was 86 (±10 SEM), and 57% of the patients were male (97/169). In total, 70 patients had a gross total resection

at the time of initial surgery, 73 had a subtotal resection, and 26 had only a biopsy before radiochemotherapy.

Of all patients enrolled, 120 had good-quality diffusion-weighted images and were included in the final analyses for this study. Exclusions were based on gross geometric distortions or low signal-to-noise ratios in the raw diffusion-weighted imaging datasets or patients with a contrast-enhancing tumor less than 0.1 cc as seen on the first MRI scan after RT + TMZ. These follow-up scans were obtained approximately 10 weeks from the time of treatment initiation (mean = 75 ± 2.6-day SEM) or approximately 4 weeks from the end of initial radiochemotherapy. At the time of last assessment, 104 of the 120 patients had died.

Treatment Paradigm
Patients were treated with 60 Gy of external beam radiation therapy (2-Gy fractions given once daily for 5 days over a 6-week period) with concomitant TMZ (75 mg/m^2 orally or intravenously for 42 consecutive days), followed by a 28-day break, and then adjuvant TMZ (150 mg/m^2 orally or intravenously for 5 consecutive days in the first 28-day cycle followed by 200 mg/m^2 orally or intravenously for 5 consecutive days in the first 28-day cycle for a maximum of 6 cycles). Diffusion and standard anatomical MRI were performed within 10 weeks after the start of RT + TMZ or within 4 weeks from the end of RT + TMZ—just before adjuvant TMZ (Figure 1). The beginning of adjuvant TMZ and the MRI evaluation were performed on the same day. This is typically the first imaging evaluation after completing RT + TMZ and is therefore an important clinical decision-making time point.

MRI
Diffusion and structural MRIs were obtained on a GE Signa Excite HDx or Lx 1.5T (GE Healthcare, Waukesha, WI); Siemens Avanto or Sonata 1.5T (Siemens Healthcare, Erlangen, Germany); or Siemens Trio, Allegra, or Verio 3T MRI system. Standard anatomical MRI consisted of pre- and postcontrast (gadolinium-diethylenetriamine pentacetic acid at a dose of 0.1 mmoL/kg body weight; Magnevist, Bayer Schering Pharma, Leverkusen, Germany) axial T1-weighted images along with precontrast axial T2-weighted and fluid-attenuated inversion recovery sequences with standard sequence parameters. Patients
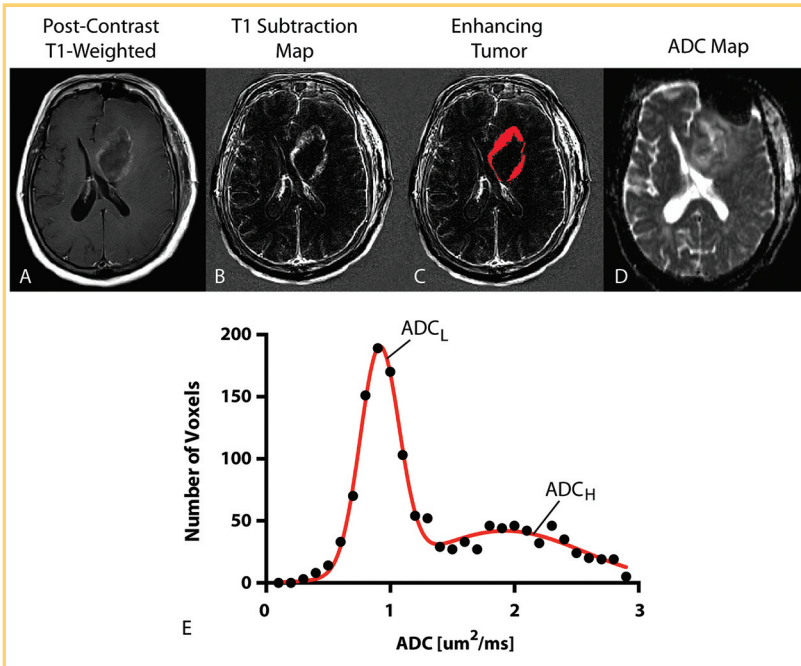
Figure 2. ADC histogram analysis. (A) Postcontrast T1-weighted image showing ring-enhancing tumor in the left frontal lobe. (B) T1 subtraction map generated from subtracting precontrast from postcontrast T1-weighted images. (C) Enhancing tumor mask extracted from T1 subtraction maps. (D) ADC map used for diffusion MRI phenotyping. (E) Resulting ADC histogram (raw data, black closed circles; double Gaussian mixed model fit, solid red line). ADC$_L$ = mean of the lower Gaussian distribution estimated the double Gaussian mixed model fit. ADC$_H$ = mean of the higher Gaussian distribution estimated from the double Gaussian mixed model fit.

also received diffusion-weighted images with an echo/repetition time = 80 to 120 ms/>5000 ms, matrix size = 128 × 128, slice thickness = 3 mm with no interslice gap, and b values of 0 and 1000 s/mm^2 in 3 orthogonal directions. ADC maps were calculated for each image voxel as ADC$(x, y, z) = -1/1000 \cdot \ln[S(x, y, z)/S_0(x, y, z)]$, where $S(x, y, z)$ is the signal intensity of the voxel at coordinate (x, y, z) with $b = 1000$ s/mm^2 and $S_0(x, y, z)$ is the signal intensity at voxel (x, y, z) with $b = 0$ s/mm^2.

ADC Histogram Analysis
ADC histogram analysis was performed using previously described techniques (13-15). Briefly, contrast-enhancing tumor regions were segmented on T1 subtraction images calculated by subtracting precontrast from postcontrast T1-weighted images (22). ADC characteristics from within enhancing regions were then extracted. A double Gaussian mixed model was used to describe the ADC histogram using nonlinear regression, where ADC$_H$ reflects the mean ADC in the larger of the two Gaussian distributions and ADC$_L$ is the mean ADC value of the lower Gaussian distribution (Figure 2). Both ADC$_L$ and ADC$_H$ were used as the primary imaging biomarker for the current study using GraphPad Prism version 6 (GraphPad Software, Inc., La Jolla, CA).

Definition of Tumor Progression
Progression was defined prospectively by the treating neuro-oncologists if subsequent scans showed an increase in imaging-evaluable tumor (≥25% increase in the sum of enhancing lesions, new enhancing lesions > 1 cm^2, an unequivocal qualitative increase in nonenhancing tumor, or an unequivocal new area of noncontrast-enhancing tumor). Patients were required to have a stable or decreasing contrast agent dose before partial or complete response could be determined. In addition, patients who required an increased dosage of steroids to maintain neurologic function, even when anatomical images showed no worsening, were considered to be stable but required early

reevaluation. Patients who experienced significant neurologic decline were also declared to have progressed at the time of irreversible decline. Landmark PFS was defined as the time between the MRI scan following completion of RT + TMZ and progression. Landmark OS was defined as the time between the MRI scan and death.

Statistical Analyses
Receiver operating characteristic (ROC) analysis was used to determine whether a low ADC$_L$ could identify patients who progressed within 6 months from starting adjuvant TMZ (i.e., PFS6) and patients who died within 12 months from starting adjuvant TMZ (e.g., OS12) using area under the ROC curve (AUC) as a measure of performance. An ADC$_L$ value of 1.0 μm^2/ms and ADC$_H$ value of 1.6 μm^2/ms were chosen as the primary biomarkers of interest because these values were near the median of the patient distribution and found to have the highest likelihood ratio (sensitivity/[1 − specificity]) for both PFS6 and OS12. This cutoff was then used to stratify PFS and OS using both log-rank analysis on Kaplan-Meier data and multivariate Cox regression analysis using age as an additional covariate. A P value less than .05 was considered statistically significant, and a P value less than .10 was considered trending toward significance.

RESULTS
ROC Analysis
Results suggest ADC$_L$ is a significant predictor of patients that will progress within 6 months of starting adjuvant TMZ (Figure 3A; ROC AUC = 0.68 ± 0.053 SEM, P = .0011); however, ADC$_H$ was not a significant predictor of progression by 6 months (Figure 2A; ROC AUC = 0.5768 ± 0.057 SEM, P = .2187). A threshold of ADC$_L$ < 1.0 μm^2/ms had a low sensitivity (34%) and high specificity (90%) for identifying patients that would progress within 6 months, meaning a high proportion of patients with low ADC$_L$ after RT + TMZ will progress early after starting adjuvant TMZ (Figure 3B; t test, P = .027). (For reference, an
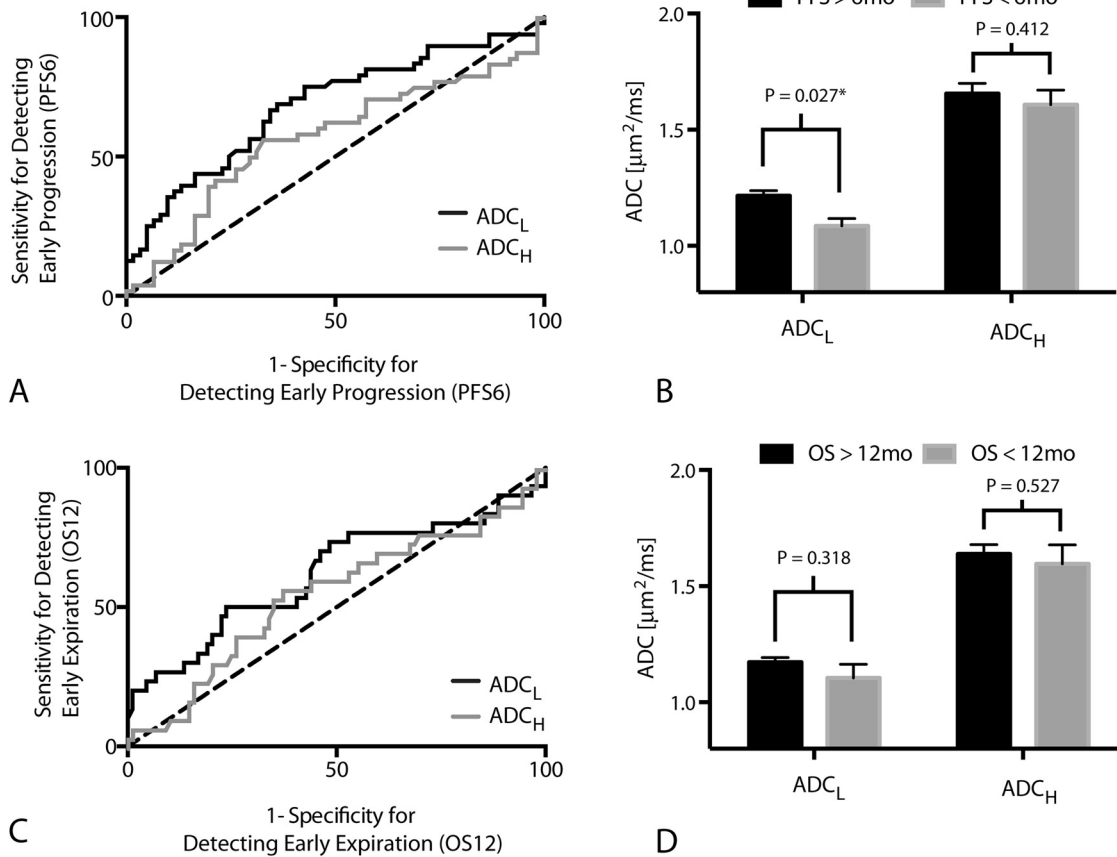
Figure 3. ROC curves. (A) ROC curve showing the sensitivity and specificity of ADC_L and ADC_H in detecting patients who progressed within 6 months of starting adjuvant TMZ (PFS6) (ADC_L: ROC AUC = 0.6820 ± 0.05252 SEM, P = .0011; ADC_H: ROC AUC = 0.5768 ± 0.057 SEM, P = .2187). (B) ADC_L and ADC_H measurements for individual tumors categorized based on progression before or after 6 months from the start of adjuvant TMZ (PFS6). Significant differences in ADC_L (t test, P = .027) but not ADC_H (t test, P = .412) were observed between patients progressing before and after 6 months from the start of adjuvant TMZ. (C) ROC curve showing the sensitivity and specificity of ADC_L and ADC_H in detecting patients who died within 12 months of starting adjuvant TMZ (OS12) (ADC_L; ROC AUC = 0.6176 ± 0.06551 SEM, P = .0547; ADC_H: ROC AUC = 0.55 ± 0.064 SEM, P = .4104). (D) ADC_L and ADC_H measurements for individual tumors categorized based on death before or after 12 months from the start of adjuvant TMZ (OS12). No significant differences were observed in measurements of ADC_L (t test, P = .318) or ADC_H (t test, P = .527) when patients were stratified by OS12.

$ADC_L < 1.2$ μm^2/ms used in previous studies showed a sensitivity of 71% and specificity of 57% for PFS6.)

ADC_L also trended toward being a significant predictor of OS12 (Figure 3C; ROC AUC = 0.62 ± 0.066 SEM, P = .0547), whereas ADC_H did not predict OS12 (Figure 3C; ROC AUC = 0.55 ± 0.064 SEM, P = .4104). ADC_L showed a relatively low sensitivity (33%) but high specificity (82%) of predicting OS12 when using $ADC_L < 1.0$ μm^2/ms for patient stratification. (For $ADC_L < 1.2$ μm^2/ms, sensitivity/specificity = 73%/48%.)

Progression-Free Survival

Patients with an $ADC_L < 1.0$ μm^2/ms had a significantly shorter PFS compared with the rest of the patients (Figure 4A; log-rank, $P < .0001$). Median PFS for patients exhibiting a low ADC_L (< 1.0 μm^2/ms) was 156 days compared with a median PFS of

288 days for patients with a high ADC_L (> 1.0 μm^2/ms). Similarly, patients with an $ADC_H < 1.6$ μm^2/ms also demonstrated a significantly shorter PFS compared with the rest of the patients (Figure 4B; log-rank, $P = .0012$), with a median PFS of 173 days compared with 304 days for patients with an $ADC_H > 1.6$ μm^2/ms. A Cox multivariate regression that examined the effects of age, ADC_L, and ADC_H on PFS confirmed that ADC_L was a significant predictor of PFS (Cox: HR = 0.11 [95% CI: 0.03, 0.39], $P = .0006$) and age trended toward significance (Cox: HR = 1.02 [95% CI: 1.00, 1.04], $P = .0521$). No association between ADC_H and PFS was observed when accounting for age and ADC_L (Cox regression, $P = .9498$). No differences in ADC_L were observed between O6-methylguanine methyltransferase methylated and unmethylated tumors (t test, $P = .38$), but methylated tumors had significantly higher values of ADC_H (t
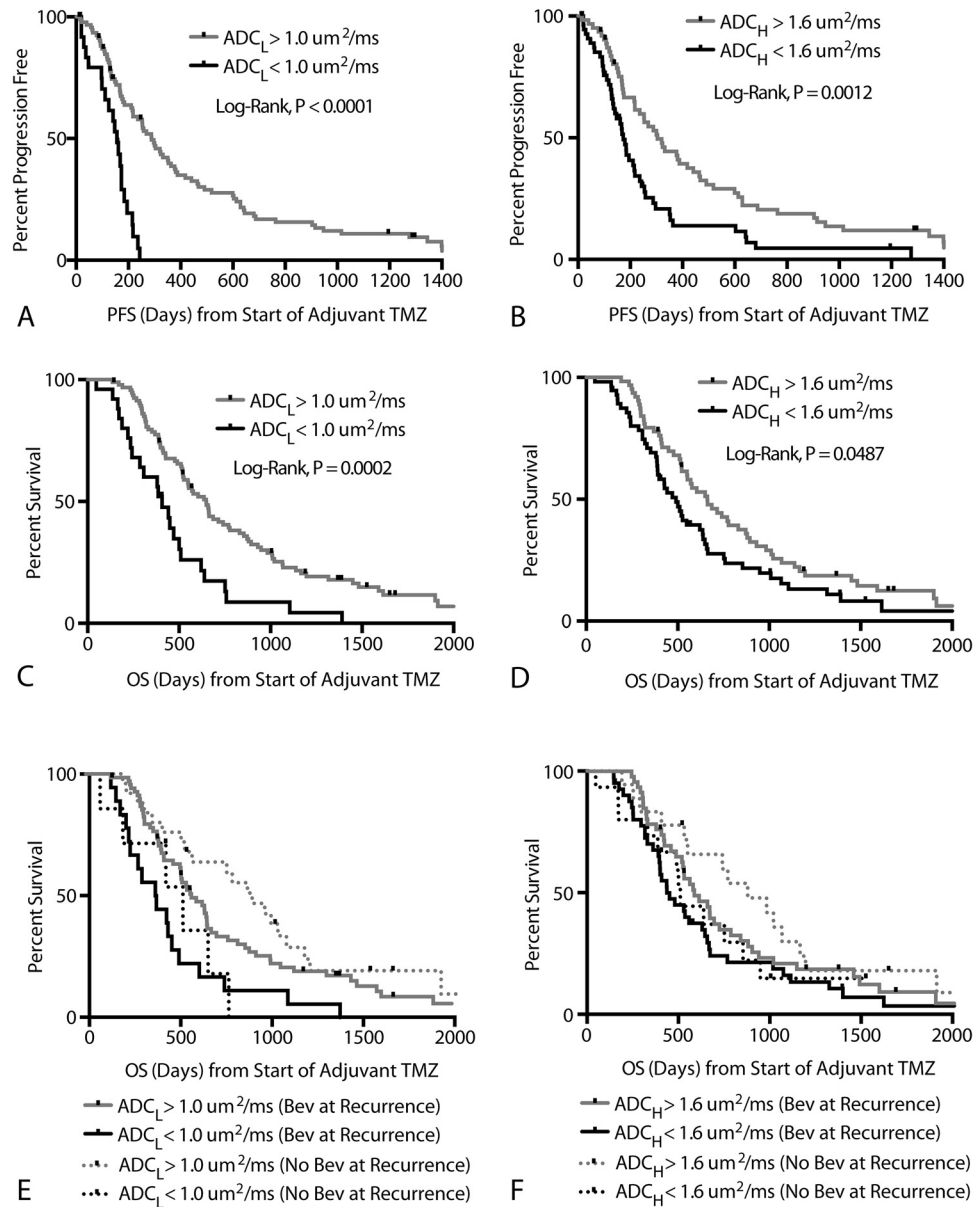
Figure 4. Progression-free and overall survival. (A) Kaplan-Meier curves showing significantly lower PFS in patients with $ADC_L < 1.0 \ \mu m^2/ms$ (log-rank, $P < .0001$; Cox multivariate, $P = .0002$). (B) Kaplan-Meier curves showing significantly lower PFS in patients with $ADC_H < 1.6 \ \mu m^2/ms$ in univariate analysis (log-rank, $P = .0012$); however, ADC_H was not significant in multivariate analysis (Cox multivariate, $P = .9498$). (C) Kaplan-Meier curves showing significantly lower OS in patients with $ADC_L < 1.0 \ \mu m^2/ms$ (log-rank, $P = .0002$; Cox multivariate, $P = .0487$). (D) Kaplan-Meier curves showing significantly lower OS in patients with $ADC_H < 1.6 \ \mu m^2/ms$ in univariate analysis (log-rank, $P = .0487$) but not when accounting for age and ADC_L (Cox multivariate, $P = .5478$). (E) Kaplan-Meier curves showing differences in OS based on ADC_L higher or lower than $1.0 \ \mu m^2/ms$ for both bevacizumab-naïve (log-rank, $P = .0130$) and bevacizumab-treated (log-rank, $P = .0029$) patients at recurrence. No differences in OS were observed between patients treated with bevacizumab and those who were not within high ADC_L (log-rank, $P = .1977$) or low ADC_L (log-rank, $P = .8959$) groups. (F) Kaplan-Meier curves showing no differences in OS based on ADC_H higher or lower than $1.6 \ \mu m^2/ms$ for both bevacizumab-naïve (log-rank, $P = .1330$) and bevacizumab-treated (log-rank, $P = .1510$) patients at recurrence.

test, $P = .0443$; mean ADC_H for methylated $= 1.50$ $\mu m^2/ms$; mean ADC_H for unmethylated tumors $= 1.72$ $\mu m^2/ms$).

Overall Survival

Patients with an $ADC_L < 1.0$ $\mu m^2/ms$ had a significantly shorter OS compared with patients who had a higher ADC_L (Figure 4C; log-rank, $P = .0002$), with median OS for patients with a low ADC_L (< 1.0 $\mu m^2/ms$) around 407 days compared with 648 days for patients with a high ADC_L (> 1.0 $\mu m^2/ms$). Similarly, patients with an $ADC_H < 1.6$ $\mu m^2/ms$ also had a significantly shorter OS compared with patients who exhibited a higher ADC_H (Figure 4D; log-rank, $P = .0487$), with median OS for patients with a low ADC_H around 491 days compared with 662 days for patients with a high ADC_H. Cox multivariate regression confirmed that both age (Cox: HR $= 1.03$ [95% CI: 1.01, 1.05], $P = .001$) and ADC_L (Cox: HR $= 0.31$ [95% CI: 0.09, 0.98], $P = .047$) were correlated with OS. ADC_H was not significantly associated with OS when accounting for age and ADC_L (Cox, $P = .5478$).

Significant OS differences were observed between high and low ADC_L in both patients who received bevacizumab at first recurrence ($n = 87$; log-rank, $P = .003$) and those who did not ($n = 33$; log-rank, $P = .01$) (Figure 4E). No differences were observed between high and low ADC_H in patients who received bevacizumab at first recurrence (log-rank, $P = .1510$) and those who did not (log-rank, $P = .1330$) (Figure 4F). No differences in OS were observed between patients treated with bevacizumab and those who were not within high ADC_L (log-rank, $P = .20$) or low ADC_L (log-rank, $P = .90$) groups.

DISCUSSION

Diffusion MRI measures of ADC have been shown to be correlated with both tumor cellularity (19, 23-25) and mitotic activity (26). Therefore, successful radiochemotherapy would be expected to result in a relatively higher amount of tumor cell destruction, leading to an increase in the diffusivity of water within the tumor as a result of the lack of restrictions to diffusion from structures such as cell membranes. Tumors with a low ADC following combined RT + TMZ, on the other hand, may consist of a more cellular, aggressive, possibly more treatment-resistant tumor phenotype. Results from this study support this hypothesis, suggesting patients with an $ADC_L < 1.0$ $\mu m^2/ms$ in contrast-enhancing tumors have a significantly shorter PFS and OS after starting adjuvant TMZ compared with other patients.

Previous studies using ADC histogram analysis have shown that tumor ADC_L values greater than 1.2 $\mu m^2/ms$ have a significantly longer PFS and OS in recurrent GBM treated with bevacizumab (13-15, 27). Using the threshold of 1.0 $\mu m^2/ms$, we did not observe any difference in OS between patients treated with bevacizumab and those who were not. However, we did observe this trend at recurrence when using a threshold of 1.2 $\mu m^2/ms$ (data not shown), but this threshold was not significant when

used for evaluating adjuvant TMZ and thus was not used in this study. Together, these results may suggest patients with a low ADC_L (< 1.0 $\mu m^2/ms$) after RT + TMZ are likely to be nonresponsive to any subsequent therapies, including bevacizumab or additional chemotherapies; patients with a high ADC_L (> 1.2 $\mu m^2/ms$) are likely to respond favorably to bevacizumab at first recurrence; and patients with an intermediate ADC_L (1.0 $\mu m^2/ms < ADC_L < 1.2$ $\mu m^2/ms$) may benefit from subsequent chemotherapy before treatment with bevacizumab.

There are a few limitations to this study that should be noted. It is important to point out that there was a potential selection bias because only patients who successfully completed surgical resection and RT + TMZ with a measurable contrast-enhancing tumor (>0.1 cc) were eligible for ADC histogram analysis. In addition, it is conceivable that some patients determined to have early progression after completing RT + TMZ actually had pseudoprogression, or treatment-related changes in vascular permeability that mimic radiographic changes similar to treatment failure or tumor growth. The addition of multimodal imaging techniques, including perfusion MRI (28), may have allowed for a more accurate delineation of pseudoprogression from true progression. Despite this potential confounding variable, we found significant differences in both PFS and OS in all patients based on diffusion characteristics as well as in patients with a PFS greater than 3 months from the end of RT + TMZ, where the incidence of pseudoprogression is likely to be highest. Moreover, this study involved acquiring diffusion MRIs using a variety of MRI systems and field strengths for the purpose of mimicking a clinical trial environment. Recent studies have shown that errors in ADC measurements vary nonlinearly from the scanner isocenter and that different MRI systems have different degrees of nonlinearity (29). Thus, this study would have benefited from the use of a temperature-controlled water phantom to account for system-specific errors in ADC measurements.

In summary, this study demonstrates that diffusion characteristics obtained using ADC histogram analysis can be used to predict PFS and OS after completing RT + TMZ and before adjuvant TMZ therapy. Results suggest that patients with an $ADC_L < 1.0$ $\mu m^2/ms$ are at increased risk for early progression and early death, indicating that ADC histogram analysis may be useful for patient-risk stratification after completing RT + TMZ. Future studies aimed at integrating ADC histogram analysis into clinical decision making as well as identifying biological correlates of diffusion characteristics are warranted.

Conflicts of Interest: Drs. Timothy F. Cloughesy, Albert Lai, Whitney B. Pope, and Benjamin M. Ellingson are paid consultants for Genentech, Inc., and Hoffman-La Roche, Ltd. Drs. Ellingson and Pope are also a paid consultant for MedQIA, LLC.

REFERENCES

1. Stupp R, Mason WP, van den Bent MJ, Weller M, Fisher B, Taphoorn MJ, Belanger K, Brandes AA, Marosi C, Bogdahn U, Curschmann J, Janzer RC, Ludwin SK, Gorlia T, Allgeier A, Lacombe D, Cairncross JG, Eisenhauer E, Mirimanoff RO. European Organisation for Research and Treatment of Cancer Brain Tumor and Radiotherapy Groups, National Cancer Institute of Canada Clinical Trials Group. Radiotherapy plus concomitant and adjuvant temozolomide for glioblastoma. N Engl J Med. 2005;352(10):987–996.

2. Park CK, Lee SH, Kim TM, Choi SH, Park SH, Heo DS, Kim IH, Jung HW. The value of temozolomide in combination with radiotherapy during standard treatment for newly diagnosed glioblastoma. J Neurooncol. 2013;112(2):277–283.

3. Sher DJ, Henson JW, Avutu B, Hochberg FH, Batchelor TT, Martuza RL, Barker FG 2nd, Loeffler JS, Chakravarti A. The added value of concurrently administered temozolomide versus adjuvant temozolomide alone in newly diagnosed glioblastoma. J Neurooncol. 2008;88(1):43–50.

4. Chaudhry NS, Shah AH, Ferraro N, Snelling BM, Bregy A, Madhavan K, Komotar RJ. Predictors of long-term survival in patients with glioblastoma multiforme: advancements from the last quarter century. Cancer Invest. 2013;31(5):287–308.

5. Kumar N, Kumar P, Angurana SL, Khosla D, Mukherjee KK, Aggarwal R, Kumar R, Bera A, Sharma SC. Evaluation of outcome and prognostic factors in patients of glioblastoma multiforme: a single institution experience. J Neurosci Rural Pract. 2013;4(suppl 1):S46–S55.

6. Parks C, Heald J, Hall G, Kamaly-Asl I. Can the prognosis of individual patients with glioblastoma be predicted using an online calculator? Neuro Oncol. 2013;15(8):1074–1078.

7. Mazaris P, Hong X, Altshuler D, Schultz L, Poisson LM, Jain R, Mikkelsen T, Rosenblum M, Kalkanis S. Key determinants of short-term and long-term glioblastoma survival: a 14-year retrospective study of patients from the Hermelin Brain Tumor Center at Henry Ford Hospital. Clin Neurol Neurosurg. 2014;120:103–112.

8. Ellingson BM, Lai A, Harris RJ, Selfridge JM, Yong WH, Das K, Pope WB, Nghiemphu PL, Vinters HV, Liau LM, Mischel PS, Cloughesy TF. Probabilistic radiographic atlas of glioblastoma phenotypes. AJNR Am J Neuroradiol. 2013;34(3):533–540.

9. Marko NF, Weil RJ, Schroeder JL, Lang FF, Suki D, Sawaya RE. Extent of resection of glioblastoma revisited: personalized survival modeling facilitates more accurate survival prediction and supports a maximum-safe-resection approach to surgery. J Clin Oncol. 2014;32(8):774–782.

10. Hegi ME, Liu L, Herman JG, Stupp R, Wick W, Weller M, Mehta MP, Gilbert MR. Correlation of O6-methylguanine methyltransferase (MGMT) promoter methylation with clinical outcomes in glioblastoma and clinical strategies to modulate MGMT activity. J Clin Oncol. 2008;26(25):4189–4199.

11. Parsons DW, Jones S, Zhang X, Lin JC, Leary RJ, Angenendt P, Mankoo P, Carter H, Siu IM, Gallia GL, Olivi A, McLendon R, Rasheed BA, Keir S, Nikolskaya T, Nikolsky Y, Busam DA, Tekleab H, Diaz LA Jr, Hartigan J, Smith DR, Strausberg RL, Marie SK, Shinjo SM, Yan H, Riggins GJ, Bigner DD, Karchin R, Papadopoulos N, Parmigiani G, Vogelstein B, Velculescu VE, Kinzler KW. An integrated genomic analysis of human glioblastoma multiforme. Science. 2008;321(5897):1807–1812.

12. Yan H, Parsons DW, Jin G, McLendon R, Rasheed BA, Yuan W, Kos I, Batinic-Haberle I, Jones S, Riggins GJ, Friedman H, Friedman A, Reardon D, Herndon J, Kinzler KW, Velculescu VE, Vogelstein B, Bigner DD. IDH1 and IDH2 mutations in gliomas. N Engl J Med. 2009;360(8):765–773.

13. Ellingson BM, Sahebjam S, Kim HJ, Pope WB, Harris RJ, Woodworth DC, Lai A, Nghiemphu PL, Mason WP, Cloughesy TF. Pretreatment ADC histogram analysis is a predictive imaging biomarker for bevacizumab treatment but not chemotherapy in recurrent glioblastoma. AJNR Am J Neuroradiol. 2014;35(4):673–679.

14. Pope WB, Kim HJ, Huo J, Alger J, Brown MS, Gjertson D, Sai V, Young JR, Tekchandani L, Cloughesy T, Mischel PS, Lai A, Nghiemphu P, Rahmanuddin S, Goldin J. Recurrent glioblastoma multiforme: ADC histogram analysis predicts response to bevacizumab treatment. Radiology. 2009;252(1):182–189.

15. Pope WB, Qiao XJ, Kim HJ, Lai A, Nghiemphu P, Xue X, Ellingson BM, Schiff D, Aregawi D, Cha S, Puduvalli VK, Wu J, Yung WK, Young GS, Vredenburgh J, Barboriak D, Abrey LE, Mikkelsen T, Jain R, Paleologos NA, Rn PL, Prados M, Goldin J, Wen PY, Cloughesy T. Apparent diffusion coefficient histogram analysis stratifies progression-free and overall survival in patients with recurrent GBM treated with bevacizumab: a multi-center study. J Neurooncol. 2012;108(3):491–498.

16. Ellingson BM, Cloughesy TF, Zaw T, Lai A, Nghiemphu PL, Harris R, Lalezari S, Wagle N, Naeini KM, Carrillo J, Liau LM, Pope WB. Functional diffusion maps (fDMs) evaluated before and after radiochemotherapy predict progression-free and overall survival in newly diagnosed glioblastoma. Neuro Oncol. 2012;14(3):333–343.

17. Hamstra DA, Chenevert TL, Moffat BA, Johnson TD, Meyer CR, Mukherji SK, Quint DJ, Gebarski SS, Fan X, Tsien CI, Lawrence TS, Junck L, Rehemtulla A, Ross BD. Evaluation of the functional diffusion map as an early biomarker of time-to-progression and overall survival in high-grade glioma. Proc Natl Acad Sci U S A. 2005;102(46):16759–16764.

18. Moffat BA, Chenevert TL, Lawrence TS, Meyer CR, Johnson TD, Dong Q, Tsien C, Mukherji S, Quint DJ, Gebarski SS, Robertson PL, Junck LR, Rehemtulla A, Ross BD. Functional diffusion map: a noninvasive MRI biomarker for early stratification of clinical brain tumor response. Proc Natl Acad Sci U S A. 2005;102(15):5524–5529.

19. Chenevert TL, Stegman LD, Taylor JM, Robertson PL, Greenberg HS, Rehemtulla A, Ross BD. Diffusion magnetic resonance imaging: an early surrogate marker of therapeutic efficacy in brain tumors. J Natl Cancer Inst. 2000;92(24):2029–2036.

20. Hein PA, Eskey CJ, Dunn JF, Hug EB. Diffusion-weighted imaging in the follow-up of treated high-grade gliomas: tumor recurrence versus radiation injury. AJNR Am J Neuroradiol. 2004;25(2):201–209.

21. Castillo M, Smith JK, Kwock L, Wilber K. Apparent diffusion coefficients in the evaluation of high-grade cerebral gliomas. AJNR Am J Neuroradiol. 2001;22(1):60–64.

22. Ellingson BM, Kim HJ, Woodworth DC, Pope WB, Cloughesy JN, Harris RJ, Lai A, Nghiemphu PL, Cloughesy TF. Recurrent glioblastoma treated with bevacizumab: contrast-enhanced T1-weighted subtraction maps improve tumor delineation and aid prediction of survival in a multicenter clinical trial. Radiology. 2014;271(1):200–210.

23. Ellingson BM, Malkin MG, Rand SD, Connelly JM, Quinsey C, LaViolette PS, Bedekar DP, Schmainda KM. Validation of functional diffusion maps (fDMs) as a biomarker for human glioma cellularity. J Magn Reson Imaging. 2010;31(3):538–548.

24. Sugahara T, Korogi Y, Kochi M, Ikushima I, Shigematu Y, Hirai T, Okuda T, Liang L, Ge Y, Komohara Y, Ushio Y, Takahashi M. Usefulness of diffusion-weighted MRI with echo-planar technique in the evaluation of cellularity in gliomas. J Magn Reson Imaging. 1999;9(1):53–60.

25. Guo AC, Cummings TJ, Dash RC, Provenzale JM. Lymphomas and high-grade astrocytomas: comparison of water diffusibility and histologic characteristics. Radiology. 2002;224(1):177–183.

26. Karavaeva E, Harris RJ, Leu K, Shabihkhani M, Yong WH, Pope WB, Lai A, Nghiemphu PL, Liau LM, Chen W, Czernin J, Cloughesy TF, Ellingson BM. Relationship between [18F]FDOPA PET uptake, apparent diffusion coefficient (ADC), and proliferation rate in recurrent malignant gliomas. Mol Imaging Biol. 2015;17(3):434–442.

27. Pope WB, Mirsadraei L, Lai A, Eskin A, Qiao J, Kim HJ, Ellingson B, Nghiemphu PL, Kharbanda S, Soriano RH, Nelson SF, Yong W, Phillips HS, Cloughesy TF. Differential gene expression in glioblastoma defined by ADC histogram analysis: relationship to extracellular matrix molecules and survival. AJNR Am J Neuroradiol. 2012;33(6):1059–1064.

28. Tsien C, Galbán CJ, Chenevert TL, Johnson TD, Hamstra DA, Sundgren PC, Junck L, Meyer CR, Rehemtulla A, Lawrence T, Ross BD. Parametric response map as an imaging biomarker to distinguish progression from pseudoprogression in high-grade glioma. J Clin Oncol. 2010;28(13):2293–2299.

29. Malyarenko DI, Newitt DJ, Wilmes L, et al. Demonstration of nonlinearity bias in the measurement of the apparent diffusion coefficient in multicenter trials. [epub ahead of print] Magn Reson Med. 10.1002/mrm.25754.